the ones that characterize most electrical machines. Consecutive points in the linearization can be considered a trajectory then this methodology can be used to control a class of nonlinear systems based on multiple linearization. A synchronous generator is the base case study inthis paper.

Some interesting papers using dynamic linearization can be cited: In (Dessau, 1972) a construction of a state estimatoris given for a class of nonlinear systems S in a region of approximation Ω about the origin, the estimator is exact in Ω if the dynamically linearized approximation S^1 to S in Ω passes a rank test is proposed. In (Yu, 2016) it is proposed a data-driven iterative learning control framework for un-known nonlinear non-affine repetitive discrete-time SISO systems by applying the dynamic linearization technique. In (Bennoune, 2007) a nonlinear controller combining exact linearization technique with dynamic extension algorithm is designed.

Section 2 describes the model of a synchronous machine with its corresponding nonlinear bond graph. The linearization of the synchronous generator at an equilibrium point is proposed in Section 3. In Section 4, the dynamic linearization applied to this generator is presented. Simulation results of the linearized synchronous genera- tor at multiple points with control effects are shown in Section 6. Finally, Section 7 gives the conclusions.

2 SALIENT POLE SYNCHRONOUS MA-CHINE MODEL

Synchronous generators form the principal source of electric energy in power systems. Many large loads are driven by synchronous motors, and synchronous condensers are sometimes used as a means of providing reactive powercompensation and controlling voltage. These devices operate on the same principle and are collectively referred to as synchronous machines.

Many books and papers have used the traditional mathematical model of a synchronous machine (Anderson 1977, Kundur 1994, Smith 1993). Nevertheless in (Kamwa, 1997) a synchronous machine model considering a class of equivalent circuits with sufficient flexibility to permit the introduction of an arbitrary num- ber of damper windings. Also, the singular perturbations method is applied to synchronous machine with- out damping windings in (Duric, 1997). The transfer function block diagram model of a generator has been employed to analyze generator dynamic characteristics in (Saidy, 1996).These synchronous generators are powered by hydroelectric or thermoelectric plants (Anderson 1977, Kundur 1994). The schematic diagram of the cross-section of a synchronous generator with a pair of poles is illustrated in Fig. 1. The field winding uses direct current and producing a magnetic field that inducesvoltages in the three phases in the armature windings.

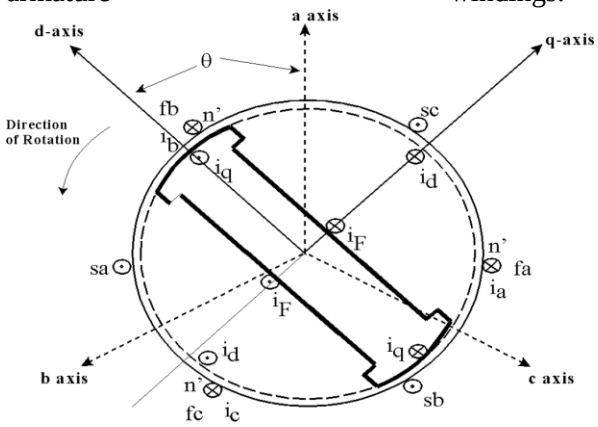

Figure 1: Schematic diagram of a three-phase synchronous machine.

The circuits used for the analysis of a synchronous generator are shown in Fig. 2. The three-phase armature winding represents the stator circuits carrying current in all three phases and the field winding describes the rotor circuit.

The following assumptions are made:

S_1 : the stator windings are sinusoidally distributed along the air-gap

S_2 : the stator slots cause no appreciable variation of the rotor inductances with rotor position

S_3 : magnetic hysteresis is negligible

S_4 : magnetic saturation effects are negligible

Consider the representation of a synchronous generator of Fig. 2.

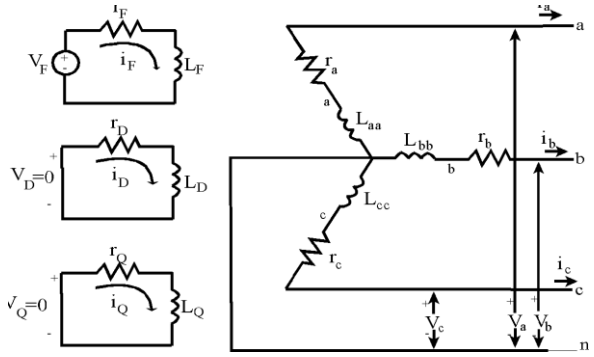

Figure 2: Stator and rotor circuits of a synchronous machine.

In this Fig. 2, we can identify the followings elements:

- a, b, c : stator phase windings. So, i_a, i_b, i_c denote the stator phase currents; υ_a, υ_b, υ_c denote the stator phase voltages, r_a, r_b, r_c denote the stator phase resistances and L_{aa}, L_{bb}, L_{cc} denote the stator phase self-inductances.
- F : field winding with i_F and υ_f denote the field cur-rent and voltage, respectively; r_F denotes the field resistance and L_F denotes the field self-inductance.
- D : d-axis damping circuit with i_D and υ_D denote the damping current and voltage on the d-axis, respectively; r_D denotes the damping resistanceon the d-axis and L_D denotes the damping self- inductances on the d-axis.
- Q : q-axis damping circuit with i_Q and υ_Q denote the damping current and voltage on the q-axis, respectively; r_Q denotes the damping resistanceon the q-axis and L_Q denotes the damping self- inductances on the q-axis.

The synchronous generator of Fig. 2 is represented by six windings are magnetically coupled. The magnetic coupling between the windings is a function of the rotorposition. The instantaneous terminal voltage υ of any winding is in the form,

$$v(t) = \pm \sum ri(t) \pm \dot{\lambda}(t) \tag{1}$$

where λ (t) is the flux linkage, r is the winding resistance and i (t) is the current with positive directions of stator currents flowing out of the generator terminals.

A great simplification in the mathematical description of the synchronous machine is obtained from the Park´s transformation. The effect of Park´s transformation is simply to transform all stator quantities from phases a, b and c into new variables the frame of reference of whichmoves with the rotor. Thus, by definition (Anderson, 1977)

$$\mathrm{i}_{0dq} = \mathrm{P}\mathrm{i}_{abc} \tag{2}$$

where the current vectors are defined as,

$$i_{0dq} = \begin{bmatrix} i_0 \\ i_d \\ i_q \end{bmatrix} \quad \text{and} \quad i_{abc} = \begin{bmatrix} i_a \\ i_b \\ i_c \end{bmatrix} \tag{3}$$

and the Park´s transformation matrix is

$$P = \begin{bmatrix} \frac{1}{\sqrt{2}} & \frac{1}{\sqrt{2}} & \frac{1}{\sqrt{2}} \\ \cos\theta & \cos\left(\theta - \frac{2\pi}{3}\right) & \cos\left(\theta + \frac{2\pi}{3}\right) \\ \sin\theta & \sin\left(\theta - \frac{2\pi}{3}\right) & \sin\left(\theta + \frac{2\pi}{3}\right) \end{bmatrix} \tag{4}$$

The angle between the d-axis and the rotor is given by

$$\theta = \omega_R t + \delta + \frac{\pi}{2} \tag{5}$$

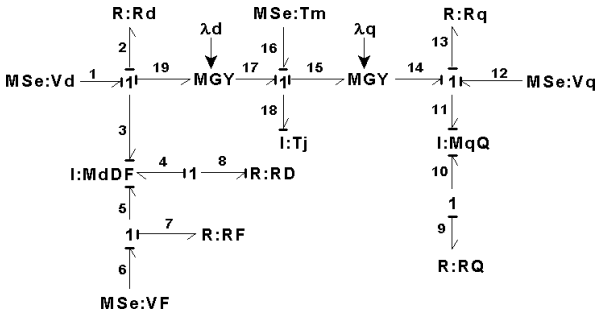

Where ω_R is the rated angular frequency in rad/s and δ is the synchronous torque angle in electrical radians. Similarly, to transform the voltages and flux linkages,

$$v_{0dq} = Pv_{abc} \tag{6}$$

$$\lambda_{0dq} = P\lambda_{abc} \tag{7}$$

The mathematical model of the synchronous generator considering the mechanical subsystem is described by

$$\begin{bmatrix} L_d & M_{dD} & M_{dF} & 0 & 0 & 0 \\ M_{dD} & L_D & M_{DF} & 0 & 0 & 0 \\ M_{dF} & M_{DF} & L_F & 0 & 0 & 0 \\ 0 & 0 & 0 & L_q & M_{qQ} & 0 \\ 0 & 0 & 0 & M_{qQ} & L_Q & 0 \\ 0 & 0 & 0 & 0 & 0 & T_J \end{bmatrix} \frac{d}{dt} \begin{bmatrix} i_d \\ i_D \\ i_F \\ i_q \\ i_Q \\ \omega \end{bmatrix} =$$

$$\begin{bmatrix} v_d \\ 0 \\ v_F \\ v_q \\ 0 \\ T_m \end{bmatrix} + \begin{bmatrix} r_d & 0 & 0 & 0 & 0 & \lambda_q \\ 0 & r_D & 0 & 0 & 0 & 0 \\ 0 & 0 & r_F & 0 & 0 & 0 \\ 0 & 0 & 0 & r_q & 0 & -\lambda_q \\ 0 & 0 & 0 & 0 & r_Q & 0 \\ \lambda_q & 0 & 0 & -\lambda_q & 0 & 0 \end{bmatrix} \begin{bmatrix} i_d \\ i_D \\ i_F \\ i_q \\ i_Q \\ \omega \end{bmatrix} \quad (8)$$

with,

$$\begin{bmatrix} \lambda_d \\ \lambda_D \\ \lambda_F \end{bmatrix} = \begin{bmatrix} L_d & M_{dD} & M_{dF} \\ M_{dD} & L_D & M_{DF} \\ M_{dF} & M_{DF} & L_F \end{bmatrix} \begin{bmatrix} i_d \\ i_D \\ i_F \end{bmatrix} \quad (9)$$

and,

$$\begin{bmatrix} \lambda_q \\ \lambda_Q \end{bmatrix} = \begin{bmatrix} L_q & M_{qQ} \\ M_{qQ} & L_Q \end{bmatrix} \begin{bmatrix} i_q \\ i_Q \end{bmatrix} \quad (10)$$

then the complete system determines a nonlinear system.

A bond graph model of this synchronous generator is shown in Fig. 3.

It can be seen that the elements that are part of the bond graph of the synchronous generator of Fig. 3 have been given in (7) and the I-fields defined by I : MdDF is described by (8) and (9) determines I : MqQ. The next section describes how to linearize systems modelled by bond graphs.

Figure 3: Nonlinear bond graph of the synchronous generator.

3 LINEARIZATION IN BOND GRAPH

When nonlinear systems defined by (Rugh, 1996)

$$\dot{x}(t) = f\left(x(t), u(t)\right) \quad \text{with} \quad x(t_0) = x_0 \quad (11)$$

with the state $x(t) \in \Re^n$ and the input $u(t) \in \Re^p$ have small disturbances around some equilibrium point can be linearized.

The linearized system is given by,

$$\dot{x}_\delta(t) = A_\delta x_\delta(t) + B_\delta u_\delta(t) \quad (12)$$

where A_δ and B_δ are the matrices of partial derivatives evaluated on the nominal trajectory, that is,

$$A_\delta = \left.\frac{\partial f}{\partial x}\right|_{(\tilde{x}(t),\tilde{u}(t))}$$
$$B_\delta = \left.\frac{\partial f}{\partial u}\right|_{(\tilde{x}(t),\tilde{u}(t))} \quad (12)$$

where $(\tilde{x}(t), \tilde{u}(t))$ is the nominal trajectory.

The linearized bond graphs are built according to the steps described in the following Procedure 1.

Procedure 1

1. In the vicinity of the nominal trajectory $(\tilde{x}(t), \tilde{u}(t))$ we have the linearization.
2. The MTF and/or MGY elements of the nonlinear bond graph are changed by TF and/or GY modulated by, $(\tilde{x}(t), \tilde{u}(t))$ respectively.
3. New causal paths are included. First, the nonlinear causal paths begin at the *(I_i, C_i)* element through one of (MTF, MGY) modulated by a state variable and arrive at (I_j, C_j) are identified. Hence, the new causal paths are constructed by replacing *(I_i, C_i)* and (I_j, C_j) by (MSe_i, MSf_i) evaluated at the nominal trajectory.

This procedure is a simplified version of the method- ology presented in (Gonzalez, 2015). Fig. 4 shows the first part of linearization process for the nonlinear bond graph of the synchronous generator shown in Fig. 3.

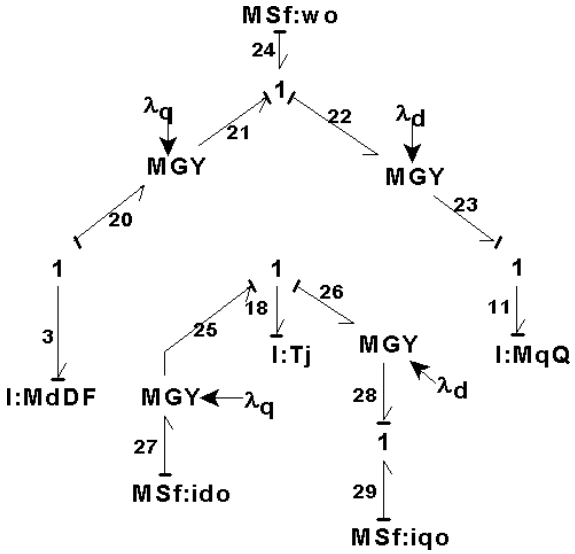

Figure 4: A step of the linearization for the synchronous generator.

Also, the nonlinear causal paths are: (3 - 19 - 17 - 18) ; (11 - 14 - 15 - 18); (18 - 17 - 19 - 3) and (18 - 15 - 14 - 11) determining the new linear causal paths that are illustrated in Fig. 5.

Figure 5: Additional causal paths for the linearization.

Joining the bond graphs of Figs. 4 and 5, the linearized bond graph of the synchronous generator is shown in Fig. 6.

The mathematical model of the linearized bond graphof Fig. 6 can be obtained according to (Gonzalez, 2015). The linearization of

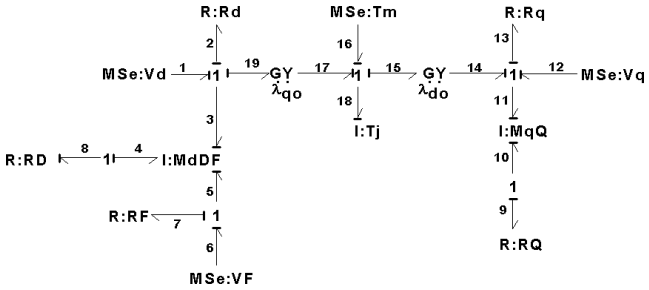

multiple operating points is presented in the next section.

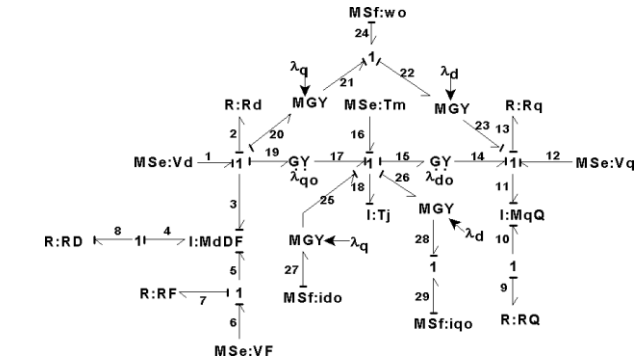

Figure 6: Linearized bond graph for the synchronousgenerator.

4 DYNAMIC LINEARIZATION

The synchronous generator linearized in the physical do-main can be shown in Fig. 7.

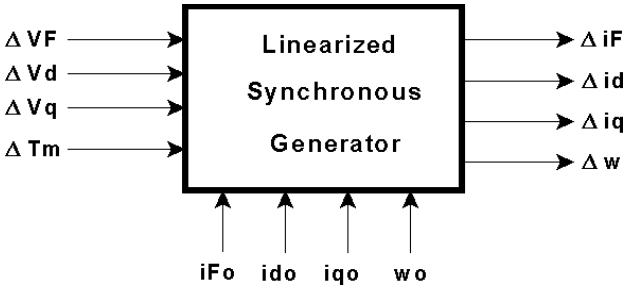

Figure 7: Scheme of the linearized synchronous generator.

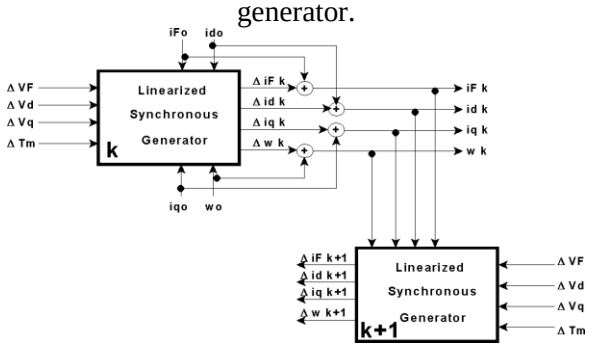

Figure 8: Dynamic linearization for the synchronous generator.

There is a set of inputs and outputs and the equilibrium point. When linearization is applied to consecutive points along a path, this linearization results in a group of linearized systems. These points of the trajectory determine the dynamic linearization. When the system is linearized at an operation point, the size of the neighborhood is considered small

and then continues to feed the state variables by changing the operation point to sweep the original signal as shown in Fig. 8.

The incremental inputs to each block determine the size of the neighborhood of that block. The blocks of Fig. 8 can be recursive with the proper programming and then a set of points that are part of a trajectory can be obtained.

5 SIMULATION RESULTS

In order to show the effectiveness of the proposed methodology to get reduced models in a bond graph approach, the performance of the state variables are depicted. The numerical parameters are the following: $V_d = 1.554V$, $V_q = 1.33$, $T_L = -10.66N \cdot m$, $r_d = 0.00077\Omega$, $r_q = 0.00077\Omega$, $r_F = 0.00021\Omega$, $r_D = 0.0049\Omega$, $r_Q = 0.0017\Omega$, $L_d = 2.2mH$, $M_{dD} = 2mH$, $M_{dF} = 2mH$, $L_D = 2.1mH$, $M_{DF} = 8.4mH$, $L_F = 2.2mH$, $L_q = 2mH$, $M_{qQ} = 1.8mH$, $L_Q = 2.1mH$ and $J = 1.8807 \times 10^5 kg \cdot m^2$. The values of the steady state are: $i_{d0} = 1.627275 \times 10^4 A$, $i_{q0} = 1.958465 \times 10^4 A$, $i_{F0} = 4.208357 \times 10^4 A$ and $w_0 = 326.7256 rad/s$.

Figs. 9, 10 and 11 show the performance of the state variables when a single step of dynamic linearization is applied. Comparing both linear and nonlinear dynamics.

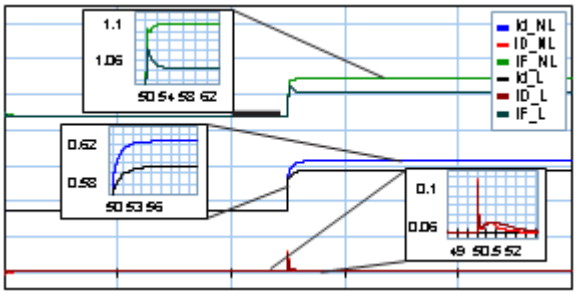

Figure 9: Electrical currents on d axis.

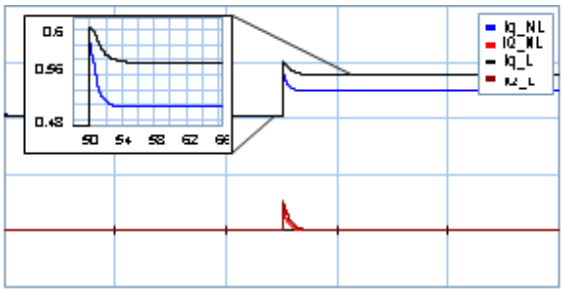

Figure 10: Electrical currents on q axis.

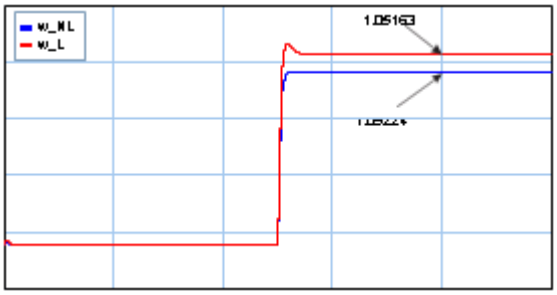

Figure 11: Angular velocity.

Now, applying 5 steps in dynamic linearization, Figs. 12, 13 and 14 illustrate the behavior of the state variables.

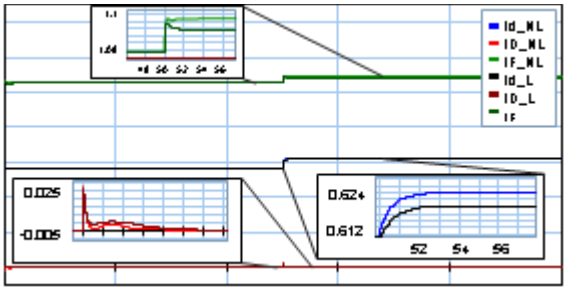

Figure 12: Electrical currents on d axis.

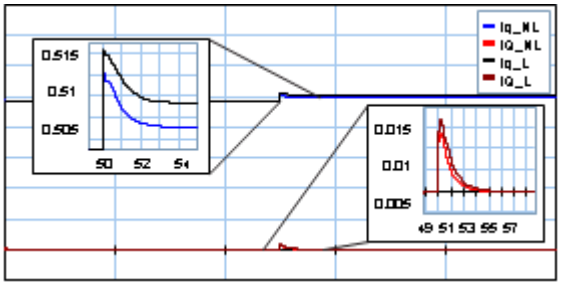

Figure 13: Electrical currents on q axis.

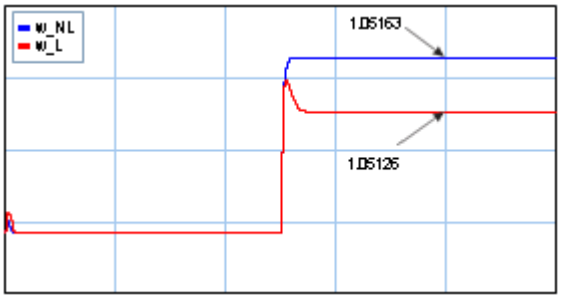

Figure 14: Angular velocity.

By increasing the number of steps of the dynamic linearization, the response of the linearized system approaches the response of the original system. Once it has been that the model of the linearized synchronous generator has a good performance compared to the nonlinear model then a control system can be ap- plied for the torque and to regulate the excitation to the generator as shown in Fig. 15.

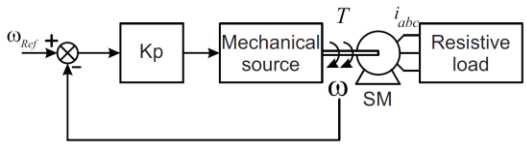

Figure 14: Closed loop system with a linearized model.

The main advantage of the scheme of Fig. 15 is that the design of the controllers will be simpler because it is a control of linearized systems.

6 CONCLUSIONS

The linearization of a synchronous generator in bond graph has been presented. The connection of a multiple linearization scheme representing a dynamic linearization in a bond graph approach is proposed. The increase in the number of steps in the dynamic linearization allows to obtain a degree of closeness with the exact values of the nonlinear model. The behavior of the generator variables with one step and 5 steps have been shown. The design of linear controllers for synchronous generators with dynamic linearization is a direct extension of the proposal made in this paper.

REFERENCES

Dean C. Karnopp, Donald L. Margolis and Ronald C. Rosenberg, *System Dynamics Modeling and Simulation of Mechatronic Systems*, Wiley, John & Sons, 2000.

W. Borutzky, *Bond graph modelling of engineering systems theory, applications and software support*, Berlin: Springer, 2011.

D. Karnopp, *Power and energy in linearized physical systems*, Journal of the Frankling Institute, 303 (1), pp. 85-98, 1977.

G. Gonzalez and R. Galindo, *A procedure to linearize a class of non-linear systems modelled by bond graphs*, Mathematical and Computer Modelling of Dynamical Systems, 21:1, 38-57, 2015.

G Gonzalez, G. Ayala, N. Barrera and A. Padilla, *Linearization of a class of non-linear systems modelled by multibond graphs*, Mathematical and Computer Modelling of Dynamical Systems, 25:3, 284- 332, 2019.

H. R. Dessau, *Dynamic Linearization and Ω-Observability of Nonlinear Systems*, Journal of Mathematical Analysis and Applications, 40, 409-417, 1972.

X. Yu, Z. Hou, A Data-Driven ILC *Framework for a Class of Nonlinear Discrete-Time Systems*, IEEE Transactions on Cybernetics, pp(99):1-1, DOI: 10.1109/TIE.2016.2636126, 2016.

A. Bennoune, A. Kaddouri and M. Ghribi, *Application of the Dynamic Linearization Technique to the Reduction of the Energy Consumption of Induction Motors*, Applied Mathematical Series, Vol. 1, 2007, no. 34, 1685-1694.

P. M. Anderson, *Power System Control and Stability*, The IOWA University Press, 1977.

P. Kundur, *Power System Stability and Control*, Mc. Graw-Hill, 1994.

John R. Smith and Meng-Jen Chen, *Three-Phase Electrical Machine Systems*, Computer Simulation, John Wiley & Sons Inc., 1993.

I. Kamwa, R. Wamkeue, X. Dai-Do, *General approaches to efficient d-q simulation and model trans- lational for synchronous machines: a recap*, Electric Power Systems Research, vol. 42, pp.173-180, 1997

Milenko Duric, Zoran Readojevic, Emilija Turkovic, *A practical approach to the order reduction of a power system model for small stability analysis*, Electric Power System Research, vol. 41, pp.13-18, 1997.

M. Saidy and F. M. Hughes, *An extended block dia- gram transfer function model of a synchronous machine*, Electric Power & Energy Systems, vol. 18, no. 2, pp. 139-142, 1996.

W. J. Rugh, *Linear System Theory*, Prentice-Hall, Upper Saddle River, NJ, 1996.